Article

Not peer-reviewed version

A Facile Growth, Optical Behavior of Organic Nonlinear Optical Crystal—4-Bromo-2-Methylbenzonitrile

Preeda P , Ganapathi Raman R * , Sakthivel Pandurengan * , Arun Thirumurugan , Suresh Sagadevan

Posted Date: 29 August 2023

doi: 10.20944/preprints202308.1898.v1

Keywords: 4B2MBN; FT-IR; FT-Raman; Photoluminescence; Antibacterial

Short Communications

A Facile Growth, Optical Behavior of Organic Nonlinear Optical Crystal—4-Bromo-2-Methylbenzonitrile

Preeda P [1], Ganapathi Raman R [1,5,*], Sakthivel Pandurengan [2,*] Arun Thirumurugan [3] and Suresh Sagadevan [4]

[1] Department of Physics, Noorul Islam Centre for Higher Education, Kumaracoil - 629180, Tamil Nadu, India.; preedapraj@gmail.com
[2] Centre for Materials Science, Science and Humanities, Faculty of Engineering, Karpagam Academy of Higher Education, Coimbatore – 641 021, Tamil Nadu, India.;sakthi1807@gmail.com
[3] Sede Vallenar, Universidad de Atacama, Vallenar 1612178, Chile; arunthiruvbm@gmail.com
[4] Nanotechnology Catalysis and Research Centre, Universiti Malaya, Kuala Lumpur 50603, Malaysia. drsureshsagadevan@um.edu.my
[5] Department of Physics, Saveetha Engineering College (Autonomous), Chennai 602 105, Tamil Nadu, India; ganapathiraman83@gmail.com
* Correspondence: ganapathiraman83@gmail.com, sakthi1807@gmail.com;

Abstract: By slowly evaporating 4-bromo-2-methylbenzonitrile at room temperature, it was possible to make a single organic nonlinear optical crystal. The grown crystal's crystalline nature was verified, and the unit cell characteristics are provided as a = 4.08Å, b = 6.61 Å, c = 28.93Å, $\alpha = 90^{o}$, $\beta = 90^{o}$, $\gamma = 90^{o}$. The functional groups of the crystal produced were identified using the FTIR and FT-Raman spectra. The UV cutoff wavelength is found at 221.6 nm, and the transparency nature of the crystal was analyzed in the optical studies. The band gap of the grown crystal was estimated using the Taucs' plot. The violet and red emissions of photoluminescence are discussed. A high dielectric constant was received at a low frequency. The TG/DTA curve shows that the grown crystal was stable up to 125.59 ^{o}C. The Kurtz-Perry powder technique was applied to confirm the Second Harmonic Generation's (SHG) nature. By using the agar diffusion method, the antibacterial property of the grown 4B2MBN crystal was determined.

Keywords: 4B2MBN; FT-IR; FT-Raman; photoluminescence; antibacterial

1. Introduction

In recent years, researchers have been doing intensive research to fabricate and develop good-quality nonlinear organic optical (NLO) materials [1]. These materials are composed of organic compounds, which contain carbon-based molecules, and are specifically designed or synthesized to exhibit enhanced nonlinear optical effects. Organic nonlinear optical crystals that are of good quality should have a large NLO coefficient, be transparent in the UV-visible range, have a high laser damage threshold, and be easy to grow in larger sizes [2]. The key advantage of using organic NLO materials is their ability to exhibit large optical nonlinearities while maintaining desirable optical and mechanical properties. They can be engineered with tailored properties such as high transparency, high damage thresholds, and a wide range of operating wavelengths, including the visible and near-infrared regions of the electromagnetic spectrum. Organic NLO materials can be categorized into various types (organic chromophores, organic polymers, Organic crystals, and organic thin films) based on their molecular structures and the underlying physical mechanisms that contribute to their nonlinear optical response.

By altering the chemical structures of organic materials, the nonlinear optical property can be tuned [3]. Molecular engineering and chemical synthesis were used to refine the properties of the organic compound [4–6]. Due to their large optical nonlinearity and flexibility in synthesis, organic nonlinear optical materials get more attention than inorganic materials [7–9]. In comparison with

 doi:10.20944/preprints202308.1898.v1

inorganic materials, organic materials have better frequency conversion efficiency because of the presence of a polarized π conjugation system. The demand for new nonlinear optical materials is due to the revolution in laser and electro-optic devices. NLO materials are also used in the areas of telecommunications, information processing, optical computing, photonics, color display, high-density optical recording, and medical diagnostics due to their potential applications as optical switches, modulators, frequency converters, and optical signal processing components [10–14].

Nitriles act as the base compounds for the synthesis of a variety of organic functional materials having triazole, imidazole, or thiadiazole moieties, and nitriles are a proximate neighbor of azoles and hydrazoles [15]. For various industrial applications, nitrile derivatives are used [16]. Compound 4-bromo-2-methylbenzonitrile (4B2MBN) has both the electron acceptor group (methyl- and -CN) group and the electron donator group (bromo-) group. There is a possibility of charge transfer through the donor-p-acceptor system, which is an additional advantage for the frequency conversion application. D. Britton reported that the 4-Bromo-2,6-dichlorobenzonitrile crystal was grown and that its crystal packing has a short distance [17]. The crystal structure of 2,6-dibromo-4-methylbenzonitrile was reported earlier by W.E. Noland [18]. No reports were presented to analyze the properties of the compound 4-bromo-2-methylbenzonitrile crystal. Hence, the target crystal is grown by the slow evaporation chemical method. Though there are various crystal growth techniques available, the chosen method for the present crystal growth has advantages, viz., cost-effectiveness and the ability to grow a novel crystal structure. This paper describes the growth and its various properties, like structural, compositional, optical, photoluminescence, thermal, dilectric, and antibacterial behaviors, of 4B2MBN crystal.

2. Materials and Methods

The chemical 4-bromo-2-methylbenzonitrile crystallized when 4B2MBN salt was mixed with the solvent ethanol. To obtain the fine, clear solution, the 4B2MBN solution was magnetically agitated at room temperature for approximately 6 hours. The solution was removed using Whatman filter paper. The transparent 4B2MBN filter-out solution was covered with a perforated layer, and the surplus solvent was then allowed to evaporate using a slow evaporation approach. After the development stage for approximately 15 days, a growth of the transparent single crystal was observed, as depicted in Figure 1.

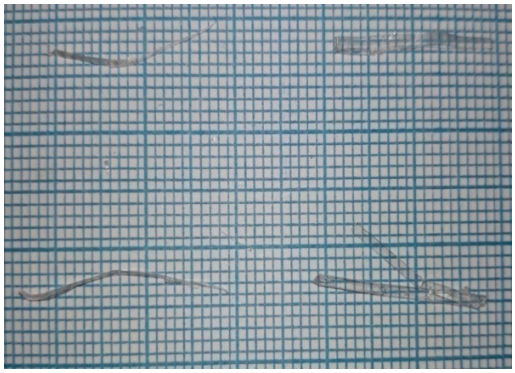

Figure 1. Grown 4B2MBN crystals.

Several ways were used to describe the 4-bromo-2-methylbenzonitrile (4B2MBN) crystal that was made. By employing the single crystal X-ray diffraction method and a BRUKER KAPPA APEX II CCD diffractometer with MoK (λ = 0.71073 Å) radiation, the unit lattice dimensions were determined. With the help of a BRUCKER D2 phaser and powder X-ray diffraction, an unknown crystalline substance was found, and using Rietveld refinement, its crystal structure was figured out. Using a Bruker APHA T spectrometer with a resolution of 0.9 cm^{-1} between 4000 and 400 cm^{-1}, the vibrational spectra were traced out. The vibrational spectrum using FT-Raman was confirmed using the ENWAVE Optronics: EzRaman N-Analyzer, with the 785nm wavelength laser beam in the region of 3200 - 100 cm^{-1}. A Systronics 2022 spectrometer was used to record the UV-visible absorption

Preprints (www.preprints.org) | NOT PEER-REVIEWED | Posted: 29 August 2023 doi:10.20944/preprints202308.1898.v1

spectrum between 200 and 800 nm. Using nitrogen and a SII Nano Technology Exstar 6300 analyzer, the TG/DTA spectrum was captured over the temperature range of 0 °C to 1300 °C. The pulsed Nd:YAG laser was utilized in conjunction with the Kurtz-Perry powder technique to examine the second harmonic production of the formed crystal. Using a Perkin Elmer LS 45 fluorometer, the emission and excitation spectra are measured in the 200–900 nm region. The Jognic 281 6B LCR meter is used to conduct the dielectric studies in the frequency range of 50 Hz to 200 kHz.

3. Results and Discussion

3.1. Single Crystal and Powder X-ray Diffraction

Single crystal X-ray diffraction and powder X-ray diffraction are two commonly used techniques in the field of crystallography to study the atomic and molecular structure of materials. While both methods involve the interaction of X-rays with a crystalline sample, they differ in terms of the nature of the sample and the type of information obtained. Single Crystal X-Ray Diffraction techniques have been carried out with MoKα (λ = 0.71073 Å) to identify the cell dimensions. The Single Crystal X-Ray Diffraction investigation reveals that 4B2MBN corresponds to the orthorhombic crystal structure with unit cell parameters a = 4.08 Å, b = 6.61 Å, c = 23.99 Å and α=β=γ = 90º and V= 782 Å^3.

3.2. FTIR Spectral Analysis

Fourier Transform Infrared (FTIR) spectroscopy is a technique used to analyze the infrared absorption or transmission of a sample. It provides information about the functional groups and chemical bonds present in a molecule, making it a powerful tool for structural identification and characterization of organic and inorganic compounds. Functional groups present in the grown 4B2MBN crystal were investigated using the FTIR and FT-Raman spectra. The recorded spectrum of FTIR was illustrated in Figure 2, and the FT-Raman spectrum was illustrated in Figure 3. Functional groups existing in 4B2MBN have been identified from the FTIR and FT-Raman spectra and are summarized in Table 1.

Table 1. Vibrational assignments of 4B2MBN.

Wavenumber (cm^{-1})		**Corresponding functional groups**
FTIR	FT-Raman	
3063, 3025		C-H stretching
2981		C-H asymmetric stretching vibration
2923		C-H symmetric stretching vibration
2784		C-H deformation overtones
2217	2332	C-N stretching vibrations
1743		C-H bending vibration
1699, 1542		C=C bending vibrations
1518	1516	C=C stretching vibration
1426	1418	C-C stretching vibration
1383	1388	CH3 symmetric bending vibration
1166	1196	C-H skeletal vibration
1111	1130, 1100	C-H symmetric deformation vibration
853		C-H bending vibration
803		C-H out of plane deformation vibration
608	608,564	C-Br stretching vibration

Preprints (www.preprints.org) | NOT PEER-REVIEWED | Posted: 29 August 2023 doi:10.20944/preprints202308.1898.v1

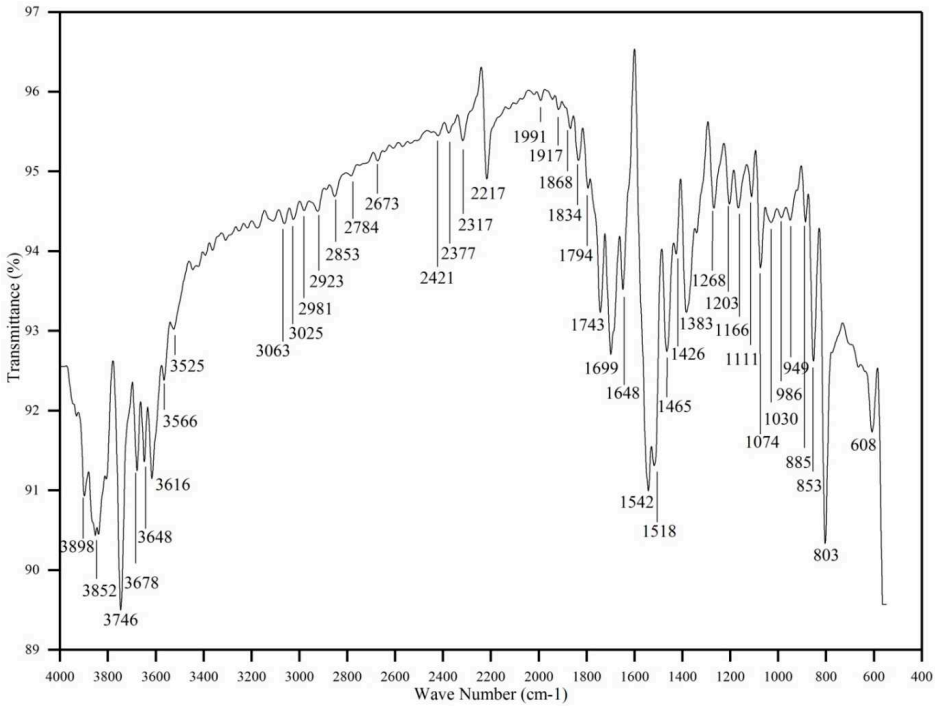

Figure 2. FTIR spectra.

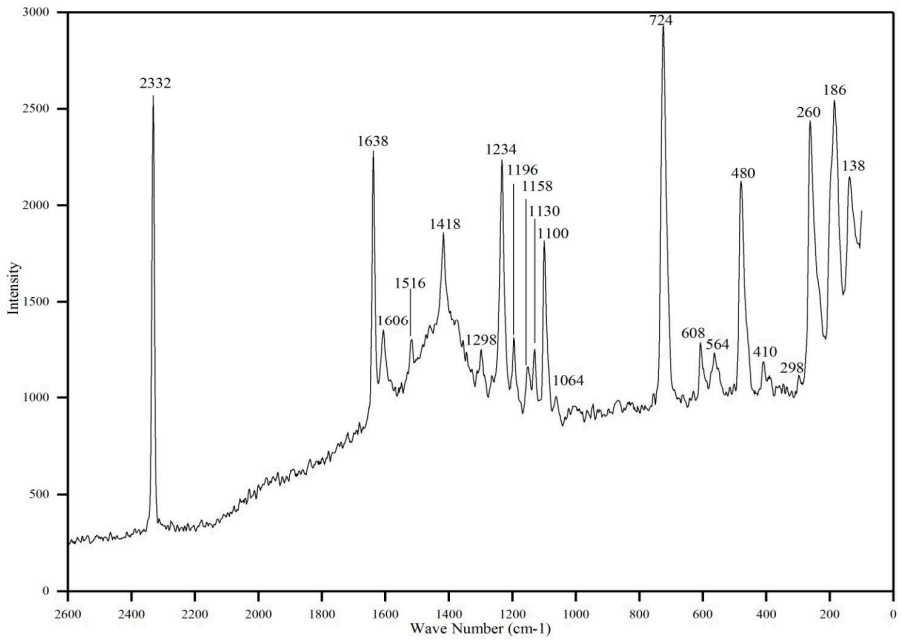

Figure 3. FT-Raman spectra.

3.3. UV- Visible Spectra: Investigation

UV-visible spectroscopy is a widely used technique for studying the interaction of ultraviolet (UV) and visible light with molecules. It provides information about the electronic transitions and absorption properties of a sample. In the application of laser frequency conversion, the prominent optical parameters are the absorbance band, transparency cutoff, and transmission range [19,20]. The optical characteristics of a 4B2MBN crystal were examined using UV-vis analysis, and the resulting spectrum is shown in Figure 4.

Preprints (www.preprints.org) | NOT PEER-REVIEWED | Posted: 29 August 2023 doi:10.20944/preprints202308.1898.v1

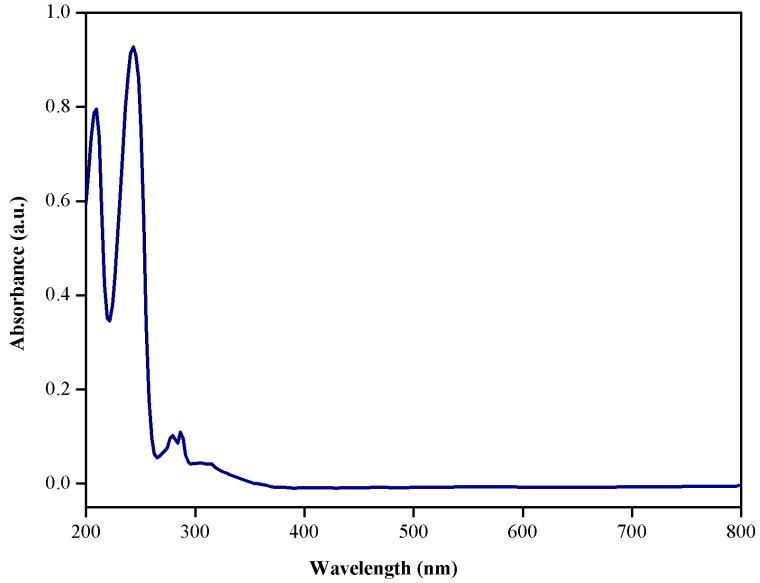

Figure 4. UV-visible spectra.

UV spectral analysis revealed the material's electronic structure and optical band gap, and the spectrum shows expert understanding of the material's electronic transition [21]. For the grown 4B2MBN crystal, the analyzed optical cutoff from the UV spectrum was observed at 264.8 nm. Since the absorption along the whole visible region was low, it substantiates the eligibility for the production of nonlinear optical devices [22]. Figure 5 depicts Tauc's plot [23] that was created between $(\alpha h\nu)^2$ and $(h\nu)$. The linear section of the picture was extrapolated to determine the band gap of the produced material, which was found to be 4.75 eV. A larger band gap and high transmittance in the visible region confirm the dielectric nature of the material [24].

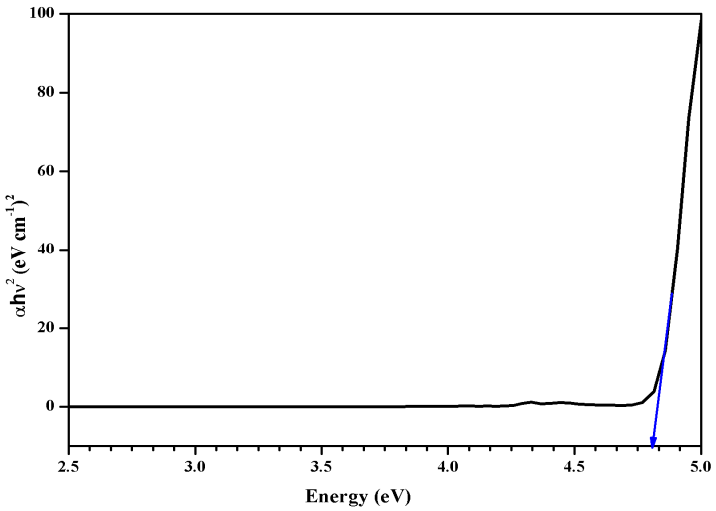

Figure 5. Tauc plot for band gap determination.

3.4. TG/DTA Studies

Thermogravimetry Differential Thermal Analysis, often known as TG/DTA, is a thermal analyzer that can simultaneously measure a sample's various thermal properties in a single experiment. The TG component measures the temperatures at which oxidation, reduction, or breakdown take place [25]. The thermogravimetric and differential thermal analyses determine the thermal characterization of the grown 4B2MBN crystal by using alumina as the reference. The TG/DTA analysis spectrum was recorded in the range of 30-800 ºC as shown in Figure 6. There was no weight loss up to 98.35 ºC in the TG spectrum. So decomposition starts from here and ends at

Preprints (www.preprints.org) | NOT PEER-REVIEWED | Posted: 29 August 2023 doi:10.20944/preprints202308.1898.v1

202.72 ºC which eventually decreases gradually to zero weight. The endothermic peaks observed at 74.1ºC and 199.82 ºC were due to decomposition. Therefore, the grown 4B2MBN crystal was stable until 98.35 ºC.

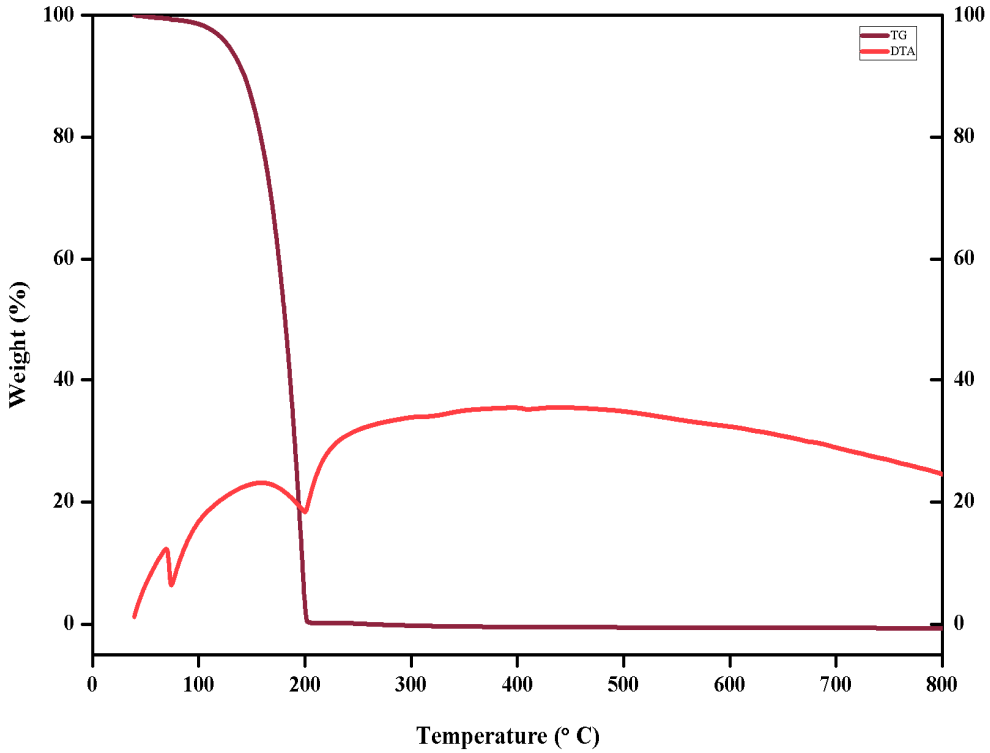

Figure 6. TG/DTA analysis.

3.5. Second harmonic generation

Second harmonic generation (SHG) is a nonlinear optical process in which two photons of the same frequency combine within a nonlinear material to generate a single photon with twice the frequency (half the wavelength) of the incident photons. It is a process that occurs in materials with non-centrosymmetric crystal structures or in certain artificially engineered structures. The 1064 nm Nd: YAG laser beam was utilized in the Kurtz-Perry technique to analyze the initial investigation of SHG conversion efficiency [26]. The grown 4B2MBN crystals are the first to be ground into small, same-size particles. Afterward, the ground particles are filled up in the invariable bore capillaries, and then they are subjected to laser radiation. It gives a second harmonic signal of 210 mV. For the reference material, the KDP crystals are finely ground to the same particle size. With the same input energy, the reference KDP crystals show a second-harmonic signal of 80 mV. Compared with the reference KDP crystal, the intensity of the bright emission of the grown 4B2MBN crystal efficiency was 2.625 times that of KDP.

3.6. Photoluminescence Spectra investigations

Photoluminescence (PL) spectroscopy is a technique used to study the emission of light from a material after it absorbs photons and undergoes a radiative recombination process. It provides information about the electronic structure, energy levels, and optical properties of the material. The photoluminescence spectra of 4B2MBN crystals are recorded, and the emission spectra are illustrated for the excitation wavelength of $\lambda = 320$ nm in Figure 7a and the excitation wavelength of $\lambda = 350$ nm in Figure 7b. Figure 7a shows the predominant emission peak at 428 nm (violet) and minor emission peaks at 647 nm (red) and 833 nm (Infrared). Figure 7b shows two peaks at 427 nm (violet) and 706 nm (Infrared). When the excitation wavelength is increased, the violet emission intensity is

Preprints (www.preprints.org) | NOT PEER-REVIEWED | Posted: 29 August 2023 doi:10.20944/preprints202308.1898.v1

substantially decreased, and the red emission is shifted to the higher wavelength side. A similar change in photoluminescence was observed in earlier research [27]. This violet emission is received from the internal part of the crystal [28] and the red emission is ascertained from the interdimeric interaction [29].

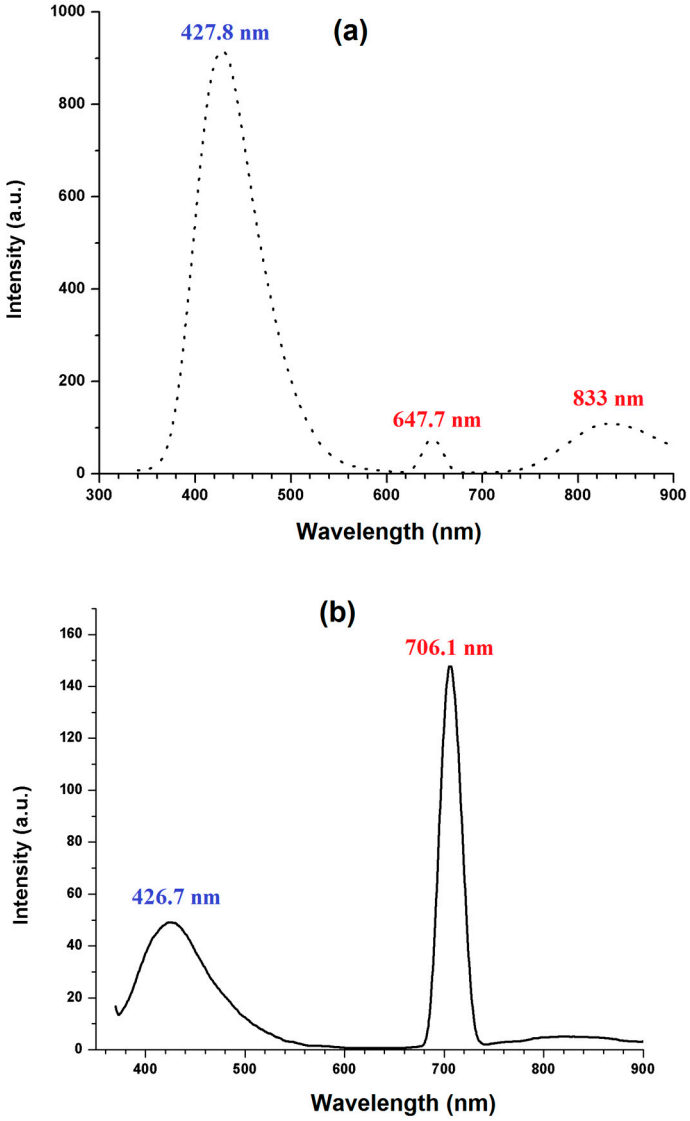

Figure 7. Photoluminescence spectra of 4B2MBN crystal (a) Excitation wavelength = 320 nm (b) Excitation wavelength = 350 nm.

3.7. Dielectric behavior

The dielectric properties of a crystal refer to its ability to store and transmit electrical energy when subjected to an electric field. The electronic structure of the crystal and how charges behave within the crystal lattice are what determine these characteristics. The dielectric and electro-optic characteristics of crystals constructed of non-conducting materials are intimately connected. To polarize the dipoles in an optical material with a high dielectric constant, you need a higher poling voltage. As a result, the refractive index may change. Polling is not required because of the organic material's weak dielectric function and low refractive index. The degree of polarization charge displacement in the crystals determines the size of the dielectric constant. Figure 8 shows the produced crystal's dielectric constant. It is greater at low frequencies and smaller as the frequency rises. Materials have high dielectric constants at lower frequencies because of the involvement of electronic, ionic, dipolar, and space charge polarizations, which vary with frequency [30]. Because

Preprints (www.preprints.org) | NOT PEER-REVIEWED | Posted: 29 August 2023 doi:10.20944/preprints202308.1898.v1

the dipole does not follow the alternating field of the electric field above a certain frequency, the dielectric constant often falls with increasing frequency before reaching a constant value. Electrical conductivity falls as the frequency of the dielectric increases [31].

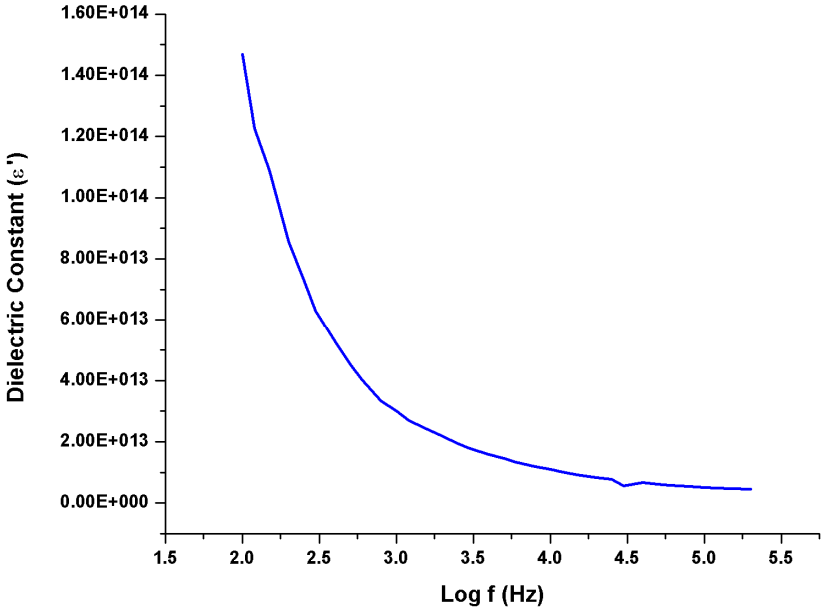

Figure 8. Dielectric behavior of 4B2MBN crystal.

3.6. Antibacterial activity

Antibacterial studies involve investigating the effectiveness of substances, compounds, or treatments in inhibiting the growth or killing bacteria. These studies aim to understand the mechanisms of action, evaluate the potency, assess the spectrum of activity, and determine the potential applications of antibacterial agents. The antimicrobial activities of the prepared 4B2MBN crystal were tested against the bacterial strains K. pneumoniae, E. coli, and Bacillus coagulans. The National Council for Clinical Laboratory Standards (NCCLS) suggested the agar-well diffusion technique be used to assess the samples' antibacterial activity. An inoculum containing 106 cfu/mL of each bacterial culture to be examined was applied to nutrient agar plates using a sterile swab moistened with the bacterial suspension. Thereafter, 8-mm-deep wells with a volume of 100 µL (25 mg/mL) of sample were drilled into the agar medium and allowed to diffuse for two hours at room temperature. The plates were subsequently given a conventional antibiotic treatment using upright, 24 h, 37 °C, imipenem (10 µg) antibiotic discs. The widths of the growth inhibition zones were measured in mm after incubation and reported on the relevant image. The zone of inhibition of 4B2MBN in E. coli, K. pneumoniae, and Bacillus coagulans is shown in Figure 9. According to the zone of inhibition, Escherichia coli exhibited the highest sensitivity, while Klebsiella pneumonia showed the least sensitivity among the tested microbes.

 doi:10.20944/preprints202308.1898.v1

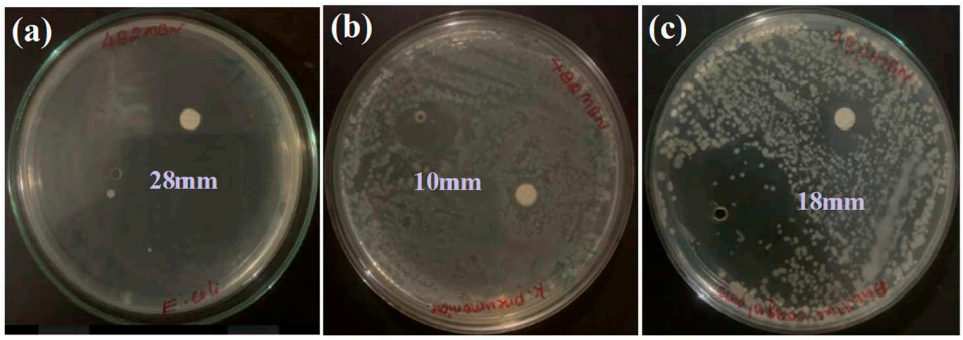

Figure 9. Antibacterial behavior of 4B2MBN crystal.

4. Conclusions

The slow evaporation technique successfully produced a single crystal of 4-bromo-2-methylbenzonitrile with excellent optical NLO transparency. Analyzing the XRD pattern has proven that the formed crystal is crystalline. The grown 4B2MBN crystal's functional groups were divided into groups using FTIR spectrum analysis. The cutoff wavelength of the grown 4B2MBN crystal was determined using the UV-Vis spectrum, and it was found to be 264.8 nm. The computed band gap energy was 4.75 eV. By looking at the TG/DTA graph, it was possible to ensure that the solvent did not exist in the 4B2MBN crystal and that there was no weight loss below 98 °C. The violet and red emissions were received through photoluminescence analysis. Because the obtained SHG efficiency of the generated crystal 4B2MBN was 2.625 times that of KDP, the developed 35D2HBA crystals can be employed as future benchmarks in optoelectronic device applications. Dielectric property is enhanced at low frequencies, and it finds application in electrical appliances. 4B2MBN showed excellent antibacterial activity against various bacterial strains (Escherichia coli, Klebsiella pneumonia, and Bacillus coagulans). Escherichia coli exhibited the highest sensitivity, while Klebsiella pneumonia showed the least sensitivity among the tested microbes.

Author Contributions: Conceptualization, methodology, software, validation, formal analysis, investigation, resources, data curation, project administration, funding acquisition, writing—original draft preparation, supervision, Preeda P. and Ganapathy Raman R; formal analysis, writing—review and editing, data curation, visualization, Sakthivel Pandurengan; Arun Thirumurugan; Suresh Sagadevan. All authors have read and agreed to the published version of the manuscript.

Funding: This research received no external funding.

Data Availability Statement: Data will be made available on reasonable request.

Acknowledgments: The authors gratefully acknowledge the crystal growth centre, Anna University, Chennai for support and utilization of facilities.

Conflicts of Interest: The authors declare no conflict of interest.

References

1. Liu X. J., Wang Z. Y., Wang X. Q., Zhang G. H., Xu S. X., Duan A. D., S. J. Zhang, Sun Z. H. and Xu D., Morphology and Physical Properties of l-Arginine Trifluoroacetate Crystals, Cryst. Growth Des. **(2008)** 8, 2270. https://doi.org/10.1021/cg7009513.
2. F. Yogam, I. Vetha Potheher, R. Jeyasekaran, M. Vimalan, A. Arockiaraj. P. Sagayaraj, Growth, thermal and Optical properties of L-asparagine monohydrate NLO single crystal, J.Them Anal Calorim. **(2013)** 114, 1153. https://doi.org/10.1007/s10973-013-3138-8.
3. A. Datta, S.K. Pati, Dipole orientation effects on nonlinear optical properties of organic molecular aggregates, J.Chem. Phys. **(2003)** 118, 8420. https://doi.org/10.1063/1.1565320.
4. E de Matos. Gomes, V. Venkataramanan, E. Nogueira, M. Belsley, F. Proença, A. Criado, M. J. Dianez, M.D. Estrada, S. Perez-Garrido, Synthesis, crystal growth and characterisation of a new nonlinear optical material — urea l-malic acid, Synth. Met. **(2000)** 115, 225. https://doi.org/10.1016/S0379-6779(00)00339-8.

5. S. Karuppusamy, K. Dinesh Babu, P. Sakthivel, Evaluation of thermal, dielectric and mechanical behavior of 4-nitrophenol crystal, Chem. Phys. Lett. **(2022)** 807, 140098. https://doi.org/10.1016/j.cplett.2022.140098.
6. S. Karuppusamy , S. Muralidharan, K. Dinesh Babu, P. Sakthivel, Thermal, dielectric, mechanical and structural behavior of 2-amino 4-methylpyridinium 4-nitrophenolate 4-nitrophenol bulk single crystal, Heliyon **(2023)** 9, E18260. https://doi.org/10.1016/j.heliyon.2023.e18260.
7. T. Pal, T. Kar, G. Bocelli, L. Rigi, Synthesis, Growth, and Characterization of l-Arginine Acetate Crystal: A Potential NLO Material, Cryst. Growth Des. **(2003)** 3, 13. https://doi.org/10.1021/cg025583y.
8. X.T. Tao, D.R. Yuan, N. Zang, M.H. Jiang, Z.S. Shao, Synthesis, Growth, and Characterization of l-Arginine Acetate Crystal: A Potential NLO Material, J. Appl. Phys. Lett. **(1992)** 60, 1415. https://doi.org/10.1021/cg025583y.
9. S. Miyata, X.T. Tao, Recent progress of organic nonlinear optics in Japan, Synth. Met. **(1996)** 81, 99. https://doi.org/10.1016/S0379-6779(96)03765-4.
10. J. Thompson, R. I. R. Blyth, M. Mazzeo, M. Anni, G. Gigli, and R. Clinigolani, White light emission from blends of blue-emitting organic molecules: a general route to the white organic light-emitting diode?, Appl. Phys. Lett. **(2001)** 79, 560–562. https://doi.org/10.1063/1.1388875.
11. N.B. Singh, T. Henningsen, R.H. Hopkins, R. Mazelsky, R.D. Hamacher, E.P. Supertzi, F.K. Hopkins, D.E. Zelmon, and O.P. Singh, Nonlinear Optical Characteristics of Binary Organic System, J. Cryst. Growth, **(1993)** 128, 976. https://doi.org/10.1016/S0022-0248(07)80081-9.
12. G. Aka, F. Mougel, F. Auge, A.K. Harari, D. Vivion, J.M. Benitez, F. Salin, D. Pelene, F. Balembois, P. Georges, A. Brun, N. Zenain, M. Jalquet, Overview of the laser and non-linear optical properties of calcium-gadolinium-oxo-borate Ca4GdO(BO3)3, J. Alloy Compounds, **(2000)** 303, 401. https://doi.org/10.1016/S0925-8388(00)00648-4.
13. C. Song, Y. Zhou, Z. Sun, T. Chen, S. Zhang, J. Luo, Crystal structure, spectroscopic studies and non-linear optical properties of 2-amino-3-nitropyridinium trichloroacetate, Cryst. Res. Technol. **(2015)** 50, 866 https://doi.org/10.1002/crat.201500056.
14. A.A. Ikizler & K. Sancak, Reaction of Ester Ethoxycarbonylhydrazones with Aliphatic Diamines, Chem. Commun. **(1995)** 60, 903. https://doi.org/10.1135/cccc19950903.
15. A.A. Ikizler & K. Sancak, Synthesis of 4-hydroxy-4,5-dihydro-1,2,4-triazol-5-ones, Monatsh Chem. **(1992)** 123, 257. https://doi.org/10.1007/BF00810474.
16. P. Preeda, R. Ganapathi Raman, P. Sakthivel, Structural, FTIR, FT-Raman, optical and nonlinear optical properties of organic nonlinear optical crystal –3,5-diisopropyl-2-hydroxybenzoic acid, Inorg. Chem. Commun. **(2022)** 146, 110120. https://doi.org/10.1016/j.inoche.2022.110120.
17. D. Britton, 4-Bromo-2,6-dichlorobenzonitrile, Acta Cryst. **(1997)** C53, 225. https://doi.org/10.1107/S0108270196012656.
18. W. E. Noland, J. E. Shudy, J. L. Rieger, Z. H. Tu and K. J. Tritch, Crystal structures of 6-dibromo-4-methyl-benzonitrile and 2,6-dibromo-4-methylphenyl isocyanide, Acta Cryst. **(2017)** E73, 1913.
19. Z. Jin, K. Nolan., C.R. McArthur, A.B.P. Lever. & C.C. Leznoff, Synthesis, electrochemical and spectroelectrochemical studies of metal-free 2,9,16,23-tetraferrocenylphthalocyanine, J. Organomet. Chem. **(1994)** 468, 205. https://doi.org/10.1016/0022-328X(94)80051-0.
20. P. Vivek. and P. Murugakoothan, Second and third order optical studies of 4- Bromoanilium hydrogen phthalate single crystal for nonlinear optical device applications, Appl. Phys. A **(2014)** 115, 1139. https://doi.org/10.1007/s00339-014-8435-y.
21. V. Mythili, T. Kanagasekaran and R. Gopala Krishnan, Investigations on nucleation kinetics, growth and characterization of sulphanilic acid single crystals, Cryst. Res. Technol. **(2007)** 42, 791. https://doi.org/10.1002/crat.200710907.
22. N. Suresh, M. Selvapandiyan, P. Sakthivel, K. Loganathan, Structural, optical, thermal, and magnetic properties of strontium nitrate doped l-Alanine crystal, Optik, **(2020)** 221, 165336. https://doi.org/10.1016/j.ijleo.2020.165336.
23. R. Abimaheshwari, P. Sakthivel & S.V. Vijayasundaram, Structural and optical investigations of ZnS quantum dots: influence of pH value, Indian J Phys. **(2022)** 96, 3755. https://doi.org/10.1007/s12648-022-02337-9.
24. T. Thilak, M. Basheer Ahamed and G. Vinitha, Third order nonlinear optical properties of Potassium dichromate single crystals by Z scan technique, Optik. **(2013)** 124, 4716. https://doi.org/10.1016/j.ijleo.2013.01.111.

25. T. Cassano, R. Tommasi, M. Ferrara, F. Babudri, G.M. Farinola. and F. Naso, Substituent-dependence of the optical nonlinearities in poly(2,5-dialkoxy-p-phenylene Vinylene) polymers investigated by Z-scan technique, Chem. Phys. **(2001)** 272, 111. https://doi.org/10.1016/S0301-0104(01)00453-0.
26. S.K. Kurtz and T.T. Perry, A Powder Technique for the Evaluation of Nonlinear Optical Materials, J. Appl. Phys. **(1968)** 39, 3798. https://doi.org/10.1063/1.1656857.
27. Y.Li, R. Hu, X. Zhang, Z. Yin, J. Qiu, Z. Yang and Z. Song, Emergence of photoluminescence enhancement of Eu3+ doped BiOCl single-crystalline nanosheets at reduced vertical dimensions, Nanoscale, **(2018)** 10, 4865. https://doi.org/10.1039/C7NR07172H.
28. A.G. Mirochnik, E. V. Fedorenko, A. A. Karpenko, D. A. Gizzatulina and V. E. Karasev, Size-dependent fluorescence of dibenzoylmethanate and ditoluylmethanate of boron difluoride, Luminescence. **(2007)** 22, 195. https://doi.org/10.1002/bio.948
29. G. Zhang, X. Zhang, L. Kong, S. Wang, Y. Tian, X. Tao, J. Yang, Anion-controlled dimer distance induced unique solid-state fluorescence of cyano substituted styrene pyridinium, Sci Rep. **(2016)** 6, 37609. https://doi.org/10.1038/srep37609.
30. M. Shakir, B. Riscob, K.K. Maurya, V. Ganesh, M.A. Wahab, G. Bhagavannarayana, Unidirectional growth of l-asparagine monohydrate single crystal: First time observation of NLO nature and other studies of crystalline perfection, J. Cryst. Growth, **(2010)** 312, 3171. https://doi.org/10.1016/j.jcrysgro.2010.07.061.
31. P. Sakthivel, S. Muthukumaran, Influence of Co^{2+} on electrical and optical behavior of Mn2+ -doped ZnS quantum dots, Opt. & Laser Technol. **(2018)** 103, 109. https://doi.org/10.1016/j.optlastec.2018.01.025.